

A simple chemical method for conversion of *Turritella terebra* sea snail into nanobioceramics

Yesim Muge Sahin^{a,b,*}, Zeynep Orman^c and Sevil Yucel^c

^aArelPOTKAM (Polymer Technologies and Composite Application and Research Center), Istanbul Arel University 34537, Turkey

^bDepartment of Biomedical Engineering, Istanbul Arel University 34537, Turkey

^cDepartment of Bioengineering, Yildiz Technical University 34220, Turkey

In this study, a sea shell was converted into bioceramic phases at three different sintering temperatures (450 °C, 850 °C, 1000 °C). Among the obtained bioceramic phases, a valuable β -TCP was produced via mechanochemical conversion method from sea snail *Turritella terebra* at 1000 °C sintering temperature. For this reason, only the bioceramic sintered at 1000 °C was concentrated on and FT-IR, SEM/EDX, BET, XRD, ICP-OES analyses were carried out for the complete characterization of β -TCP phase. Biodegradation test in Tris-buffer solution, bioactivity tests in simulated body fluid (SBF) and cell studies were conducted. Bioactivity test results were promising and high rate of cell viability was observed in MTT assay after 24 hours and 7 days incubation. Results demonstrated that the produced β -TCP bioceramic is qualified for further consideration and experimentation with its features of pore size and ability to support bone tissue growth and cell proliferation. This study suggests an easy, economic method of nanobioceramic production.

Key words: Bioactivity, Bioceramic, Bone regeneration, TCP, Mechanochemical conversion.

Introduction

Calcium-phosphate-based ceramics have been used successfully as an augment hard tissue. Among these bioceramics the most well-known ones are hydroxyapatite [HA, $\text{Ca}_{10}(\text{PO}_4)_6(\text{OH})_2$] and β -tricalcium phosphate [β -TCP, $\text{Ca}_3(\text{PO}_4)_2$] phases. HA, is a natural component of bones and teeth; thus hydroxyapatite was employed in bone defects and voids as coatings on implant materials. β -TCP is on the other hand a biocompatible, bioresorbable calcium-phosphate apatite and has been utilized for orthopedic and dental studies. β -TCP concentration plays an important role in bone regeneration by accelerating resorption speed and apatite formation. Main advantage of β -TCP is, its biodegradability which can be adjusted by modifying the composition. In the last decades, biological resources that contain calcium such as sea shells [1], bovine bone [2], corals [3] etc. have been used to produce calcium phosphate apatites for bone grafts. It is reported that sonochemical method providing a fast and easy conversion technique gives out these promising bioceramic materials [4]. Rocha et al. [5] produced HA from cuttlefish via hydrothermal method. Kang et. al. [6] produced β -TCP from the shell of *Haliotis* sp. (abalone shell) via chemical reaction between CaHPO_4 and CaO from 950 °C to 1100 °C for

3 hours. Also marine origins such as land snails (*helix pomatia*) [7], razor shells (*ensis ensis*) [8], sea snail *Cerithium vulgatum* [9] were employed to produce calcium phosphate apatites via mechanochemical method. The final method to produce bioceramics, mechanochemical method, is advantages over other hydrothermal, and microwave production methods since it does not need expensive and complex instruments and challenging conditions such as high pressure, temperature etc. Because of this reason, we suggest an easy, economic method for nanobioceramic production in the proposed study.

Materials and Methods

Turritella terebra sea snail shells, was shown in Fig. 1, were purchased in Istanbul. Shells were cleaned and dried in the vacuum furnace for a day at 100 °C to cleanse them from dirt and organic remains. They were crushed in an agate mortar by hand grinding and processed in a high energy ball mill (Retsch Planetary Ball Mill PM 400) for an hour and sieved to obtain standard powder size under 100 μm . The seashell powders were characterized by differential thermal analysis combined with thermogravimetry (DTA/TG SII6000 Exstar TG/DTA 6300, heating rate 5 K/min, in air) to obtain the exact CaCO_3 amount in the raw shell, as illustrated in Fig. 2. In order to set the exact stoichiometry of TCP, the required ortho-phosphoric acid ($\text{H}_3\text{PO}_4^{2-}$) was calculated and Ca/P ratio was

*Corresponding author:
Tel : +90-537-975-75-07
Fax: +90-212-860-04-81
E-mail: ymugesahin@arel.edu.tr



Fig. 1. *Turritella terebra* sea snail.

adjusted as 1.50 [10]. The reaction was conducted in 50 ml of distilled water on hotplate stirrer for chemical precipitation. The temperature was set to 80 °C and an equivalent amount of H₃PO₄ was added dropwise to the mixture and the reaction was conducted for 2 hours under continuous stirring.

Powders were filtered and dried in a vacuum furnace at 100 °C overnight. Finally, the synthesized powder were sintered in an oven increasing 5 °C per minute and kept at a sintering temperature of 450 °C, 850 °C and 1000 °C for 4 hours. Sample were sintered at 450 °C, 850 °C and 1000 °C will be indicated as TT450, TT850 and TT1000 respectively.

FT-IR (Shimadzu) with an ATR unit in the range of 4000 cm⁻¹-650 cm⁻¹ was used to evaluate chemical functional groups of bioceramics before and after being soaked into SBF. XRD patterns were recorded with PANalytical Xpert Pro diffractometer and the analyses were performed in a range of 10°-80° on a 2θ step of 0.02 °. Copper Kα radiation (λ = 1.5406 nm) at operating power of 30 kV and 25 mA intensity of the current were characterization parameters

Phases were identified by comparing the experimental XRD patterns depending on the Joint Committee of Powder Diffraction Standards (JCPDS) using the cards 17-0499 for Ca₂P₂O₇ and 9-0169 for β-TCP. SEM analysis was employed (Zeiss EVO® LS 10) to analyse morphological properties of the bioceramic powders before and after being soaked in the SBF. Samples were coated with gold prior of the SEM analysis by using a Sputter Coater device (Emitech K 550X) in Ar atmosphere due to amplify the secondary electrons signal. Energy Dispersive X-ray Spectroscopy (EDX) was conducted to identify the elemental composition of the samples. Specific surface area of the samples was measured with BET analysis with Tristar II 3020. The samples were degassed at 100 °C for 2 h under nitrogen purging prior of BET measurements. Pore size and pore volume were calculated using BJH adsorption method.

In vitro bioactivity of the obtained bioceramic powder was tested in SBF medium. Method of Kokubo [11]

was used for SBF which consists of inorganic ionic composition equal to human blood plasma and buffered with TRIS at a physiological pH. Each sample was pressed under 100 bar pressure for 60 seconds to achieve pellet form. Eq. 1 was used to obtain the pellet size:

$$V_s/S_a=10 \quad (\text{Eq. 1})$$

where V_s is the volume of SBF (ml) and S_a is the apparent surface area of specimen (mm²). Pellets were sintered at 1000 °C increasing temperature 10 °C per minute for 2 hours. Then samples were immersed into SBF containing falcon tubes at 37 °C and were stored in an oven at of 37 °C. SBF was renewed on 7th, 14th, 21th days. Inductively Coupled Plasma/Optical Emission Spectrometry (ICPE9000) was used to determine the level of calcium and phosphorus ion release during certain periods in SBF solution. Pellets were immersed into tris-buffer solution having a pH value of 8 and at 37 °C to analyse their degradation behaviour. pH was measured each day at an exact time, during 7 days and data was recorded. SBF and Tris analyses were conducted in duplicate and their averages were calculated.

Cell viability study was conducted by preparing concentration of 20 mg/mL (powder / DMEM-F12); 0.1 g of material was soaked in a 5 ml DMEM-F12 solution and left at 37 °C for 24 hours. The mixture was centrifuged subsequently, the supernatant passed through a 0.2 μm filter. Cell viability and cytotoxicity of the obtained bioceramic were investigated by culturing of Saos-2 osteoblast-like cells in DMEM-F12 supplemented with 10% FBS (fetal bovine serum) at 37 °C in 5% CO₂. The culture medium was replaced every two days. MTT assay was carried out according to the manufacturer's protocol (Sigma USA). Cells were seeded in a 96-well culture plate to obtain 1x10³ cells for per well. Incubation took for 24 hours, then the sample extracts were prepared with DMEM-F12 at different concentrations. After 7 days, 20 μl MTT solution (5 mg/ml) was put to each well. Following additional incubation for 4 hours, 100 μl of DMSO was added. Absorbance was measured at 540 nm with a microplate reader (Multiskan Ascent 96/384 Plate Reader).

Results and Discussion

TG/DTA Analysis

CaO content of bioceramic powder was determined by differential and gravimetric thermal analysis (TG/DGA) which indicate mass loss% of CaCO₃ corresponding to heat induced processes data (Fig. 2). The decomposition of raw powders starts at ~600 °C and finalized at ~800 °C. A 56.8% mass loss denoted at 800 °C which accompanied by decomposition of CaCO₃ and CO₂

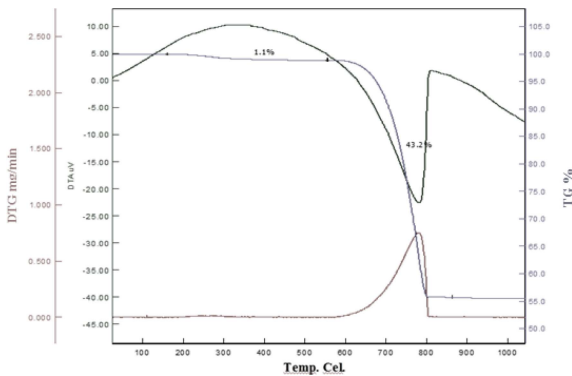
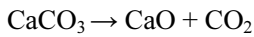


Fig. 2. DTA/TGA analysis graphics of raw powders of *Turritella terebra*.

removal. The decomposition of CaCO_3 into CaO was shown in the following chemical reaction:



Concentration of H_3PO_4 solution was calculated according to the ratio of $\text{Ca:P} = 1.5$.

X-Ray Diffraction analysis

As the produced samples were heated from 450 °C to 1000 °C, the peak height of the samples increases substantially, with an associated narrowing of the peak corresponding to increase of crystallinity. Characteristic peaks of calcium pyrophosphate ($\text{Ca}_2\text{O}_7\text{P}_2$) was observed when the samples were sintered at 450 °C and 850 °C (Fig. 3). β -TCP obtained after the heating temperature had reached to 850 °C. Peaks of β -TCP (JCPDS 09-0169) were registered at 21.9 °, 28 °, 30.9 °, 32.1 °, 34.4 ° for sample TT1000 (Fig. 4). It can be suggested that as the sintering temperature increases more intense and narrower peaks were obtained. The increase of the peak intensity can be attributed to the crystallinity increment.

Fourier transform infrared spectroscopy (FT-IR) analysis

The FTIR spectra for $\text{Ca}_2\text{P}_2\text{O}_7$ revealed various bands from the respective phosphate groups of $\text{Ca}_2\text{P}_2\text{O}_7$ as displayed in Fig 5. The bands around 1028.06 cm^{-1} for TT450 and 1026.13 cm^{-1} for TT850 was determined

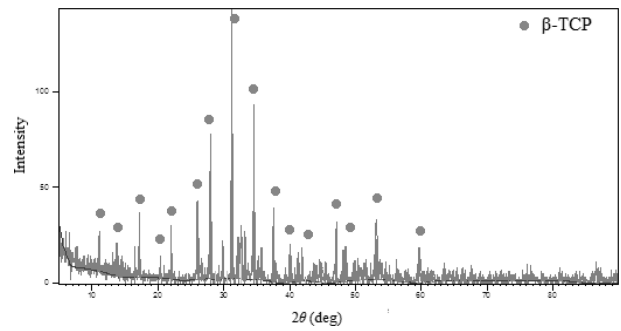


Fig. 4. XRD patterns of TT1000.

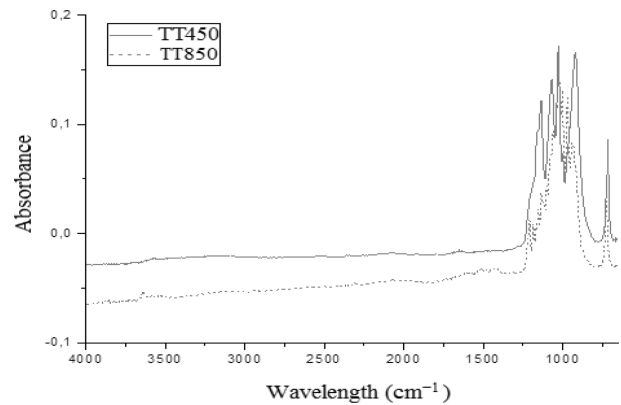


Fig. 5. FTIR spectra of TT450 and TT850.

to triply degenerate antisymmetric P-O stretching mode. P-O symmetric stretching mode was observed at 923.90 cm^{-1} for TT450 and 939.33 for TT850 [12]. FT-IR spectra of before and after heat treatment of the *Turritella terebra* raw powder at 1000 °C was shown in Fig. 6A. CO_3 bands at 1465.9, 858.32, 711.73 cm^{-1} were disappeared and PO_4 bands were appeared at 1116.78, 1078.21, 1001.06, 970.19, 943.19 for TT1000.

Samples were immersed into SBF and changes were observed regularly every week. Fig. 6B displays FT-IR spectra of samples before and after being soaked into SBF. After being soaked into SBF, phosphate group intensity increased for TT1000 and there was no evidence of CO_3^{2-} band. HA contains internal hydrogen bonds between oxygen of adjacent orthophosphate groups, resulting in the presence of HPO_4 . This band was referred as the absorption band in some biological

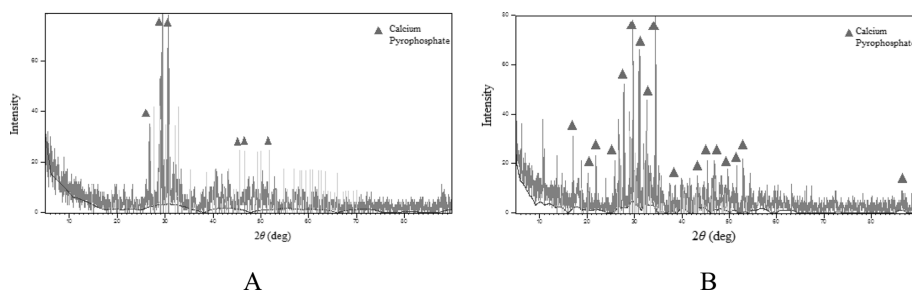


Fig. 3. XRD patterns of A) TT450 B) TT850.

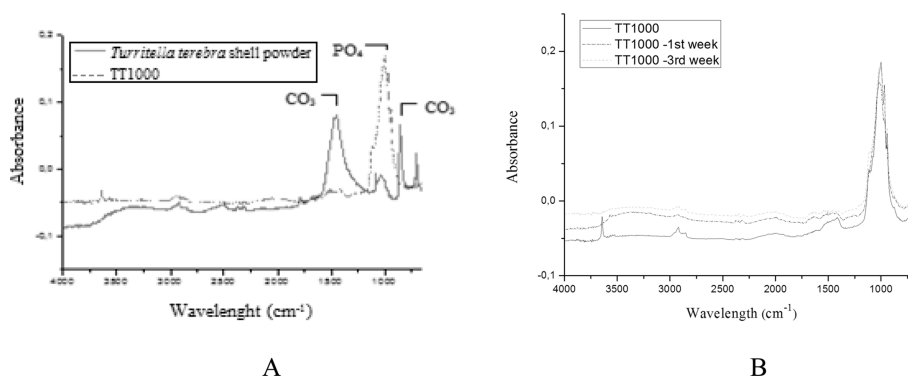


Fig. 6. A) FT-IR spectra of before and after heat treatment of the *Turritella terebra* shell powder B) TT1000: before and after being soaked in SBF.

apatites. It is suggested that typical FT-IR spectrum after being soaked into SBF, gave evidence that HA containing HPO_4^{2-} appeared [13]. These peaks can confirm that HCA (hydroxyl carbonate apatite layer) formed on the obtained bioceramic. Also broad hydroxyl peak at around 3400 cm^{-1} was observed giving clue for the HCA layer formation on the biomaterial.

BET analysis

Porous structure analysis was carried out by adsorption-desorption gas analysis. BET analysis revealed that specific surface area and pore volume decreases with increasing sintering temperature. Sintering is a heat treatment results to strength increase, reduction in surface area and generally condensation of a particle that has a high surface area. In sintering process, the formation of the bonds between the particles, the closure of the pore channels, the condensation or shrinking of the pores and the pore fusion together occurs.

Average particle diameter was calculated by following Eq. 2:

$$d = \frac{6}{\left(\text{BET surface Area in } \frac{\text{m}^2}{\text{g}} \right) \times \left(\text{Density in } \frac{\text{g}}{\text{cm}^3} \right)} \quad (\text{Eq. 2})$$

Sintering effect was evaluated for the obtained bioceramics in Table 1. It can be revealed that, as the sintering temperature increased specific surface area decreased. Average pore diameter decreased as the sintering temperature increased from $450\text{ }^\circ\text{C}$ to $850\text{ }^\circ\text{C}$

Table 1. Sintering temperature effect on specific surface area, pore volume of samples.

Origin	Sintering temperature (°C)	Specific surface area (m ² /g)	Pore volume (cm ³ /g)	Average pore diameter
<i>Turritella terebra</i>	450	11.72	0.01	6.30
	850	2.36	0.0027	4.60
	1000	1.09	0.0012	4.60

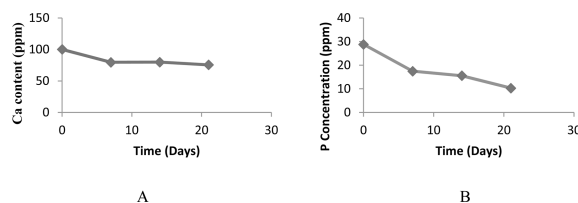


Fig. 7. A) Ca ion content of TT1000 in SBF B) P ion content of samples in SBF.

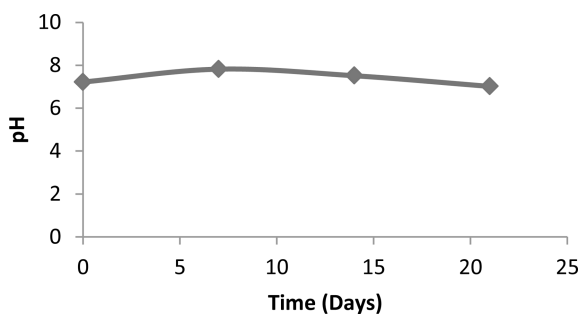


Fig. 8. pH changes of samples in a SBF solution.

and it did not change as the sintering temperature increased from $850\text{ }^\circ\text{C}$ to $1000\text{ }^\circ\text{C}$ [14].

ICP-OES analysis of simulation body fluid

Bioactivity studies of the synthesized β -TCP were investigated by SBF analyses. For this purpose HA accumulation on the produced bioceramic surfaces were analysed by ICP-OES measurements. Apatite formation occurs in SBF needs enough saturation of Ca and P ion concentration. It is a process of heterogeneous nucleation on calcium phosphate ceramic surface following the spontaneous growth of crystals. Apatite nuclei consumes Ca^{+2} and HPO_4^{2-} ions from SBF solution and it takes spherulitic shape. Positive ions in the SBF are adsorbed to surface of the calcium phosphate ceramic which leads to attraction of negative ions. Thus Ca^{2+} ions are attracted following by HPO_4^{2-} on the solid-liquid surface. Calcium and phosphate ion change was illustrated in Fig. 7. Ca level of TT1000 decreased from 100 to 79.6 ppm in the 1th week and decreased slightly until 3rd week. P concentration of TT1000 decreased drastically from 28.8

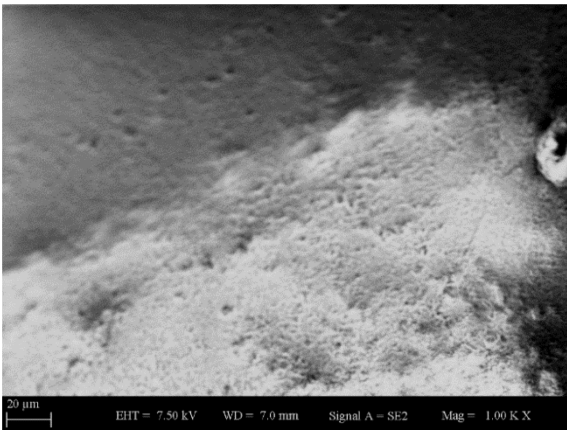


Fig. 9. SEM images of *Turrیتella terebra* shell before sieving and milling (5000x).

to 10.3 ppm. Decrease of Ca and P level in the SBF can be attributed to accumulation of the ions on the

Table 2. Ca/P ratio of the samples before and after after being soaked into SBF.

Sample	Before being soaked in SBF	Day 7 th	Day 14 th	Day 21 th
TT1000	1.88	1.95	1.35	1.52

sample surface. This is known as bone-like apatite formation and occurs when Ca and P level reach to a certain value in the solution.

pH changes give information about dissolution of the samples. Fig. 8 reveals pH change of the solution in SBF. Dissolution of β-TCP can be explained in the following chemical reaction:

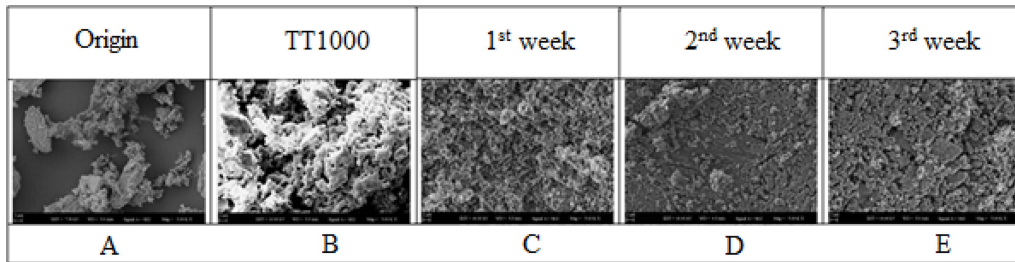
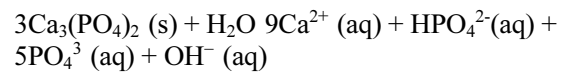


Fig. 10. SEM images of TT1000 produced from *Turrیتella terebra* sea snail before and after being soaked into SBF A) sea snail B) after sintering at 1000 °C C) after 1st week in SBF D) after 2nd week in SBF E) after 3rd week in SBF (5000x).

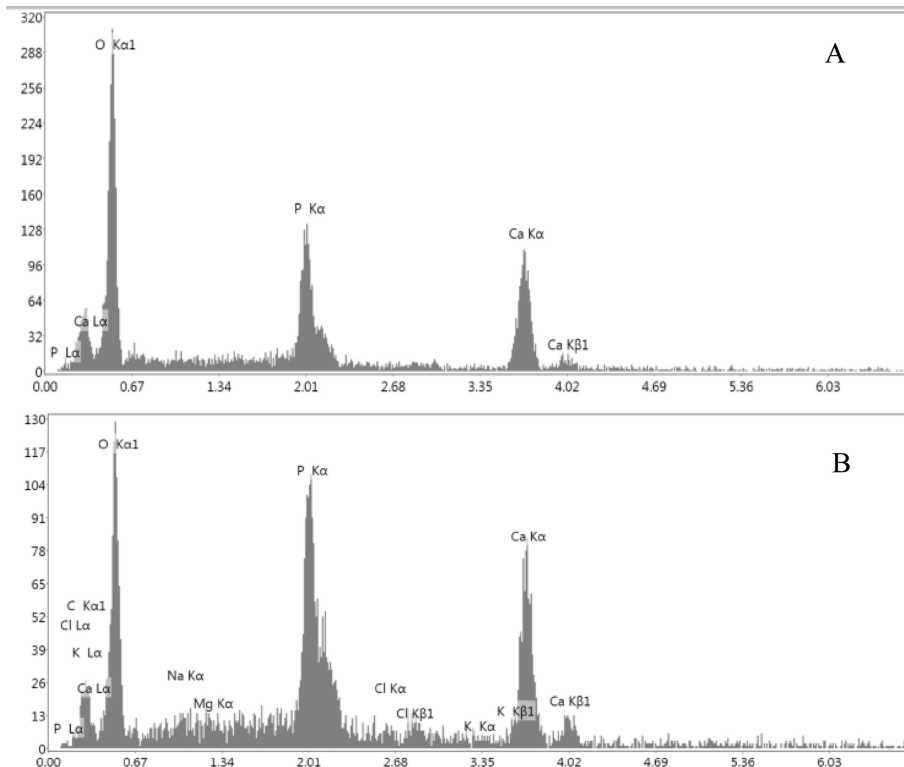


Fig. 11. A) EDX spectra of TT1000 B) TT1000 after being soaked into SBF for three weeks.

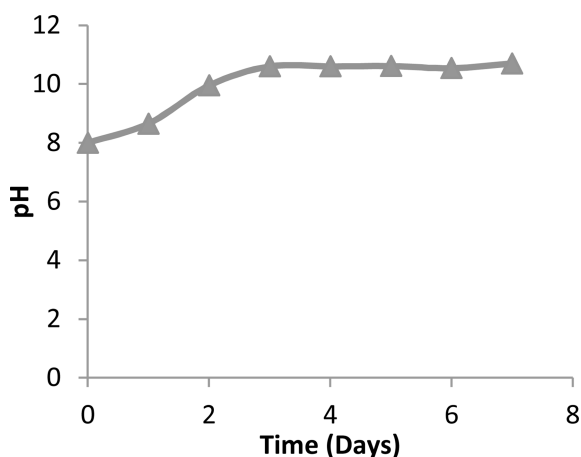


Fig. 12. pH changes of TT1000 in a Tris-buffer solution over 7 days.

H⁺ and OH⁻ ion concentrations changes as a result of dynamic nature of this dissolution process. pH increased for 7 days. After 7 days, a pH decrease was observed up to the 21th day to a final value of 7.01. The increment of pH can be attributed to HPO₄²⁻ formation in SBF.

SEM/EDX analysis

The typical microstructure at a fracture surface of the shell is exhibited in SEM image in Fig.9. A plate-like structure can be attributed largely to aragonite crystals [9].

Before and after being soaked in SBF, morphologies were monitored by SEM. SBF results revealed accumulation of HA after immersing into SBF. The surface of the material was observed to be covered with HA at the end of each week (Fig. 10). EDX analysis demonstrated that there are measurable

quantities of Cl⁻, Na⁺, Mg²⁺ in addition to Ca²⁺, P³⁻, O⁻² ions. Ca/P ratio was calculated according to EDX data (Fig. 11). It was determined that the Cl⁻, Na⁺, Mg²⁺ ions present in SBF and bonded to the bioceramic sample as a trace element.

Since β-TCP is a valuable bioceramic for tissue engineering purposes, bioactivity studies were performed for only TT1000 bioceramic sample. Ca/P ratio of the sample before and after being soaked in SBF was shown in Table 2. Ca/P ratio of TT1000 was changed from 1.35 to 1.52 between 14th and 21th days. Ca/P composition of the surface is lower than stoichiometric HA (1.67), indicates a calcium-deficient HA.

Being consistent with the ICP-OES analysis SEM results were also show the HA formation on the synthesized β-TCP bioceramics.

Before being soaked into SBF, Ca/P ratio were obtained very similar to the data for the 7 days treated sample. This result can be attributed to the formation of a thin layer of HA [15]. Within 5-10 days a subsequent degradation of TCP phase and an accumulation of HA layer on the surface of the material took place simultaneously. A slight decrease in Ca/P ratio can be attributed to this fact, where the degradation of β-TCP is much more faster than the HA accumulation. Ca/P molar ratio is 1.52 after 21 days. Ca/P ratio decrease indicates that a newly formed Ca-deficient hydroxyapatite layer accumulated on the surface of the sample [13].

pH Changes in tris-buffer solution

In vitro biodegradation behaviours were investigated in Tris solution. pH changes of samples give information of their biodegradation because Ca²⁺ and P ions release in SBF. Tris-buffer solution, [(CH₂OH)₃CNH₂], contains three active hydroxyl groups and can be stabilized by

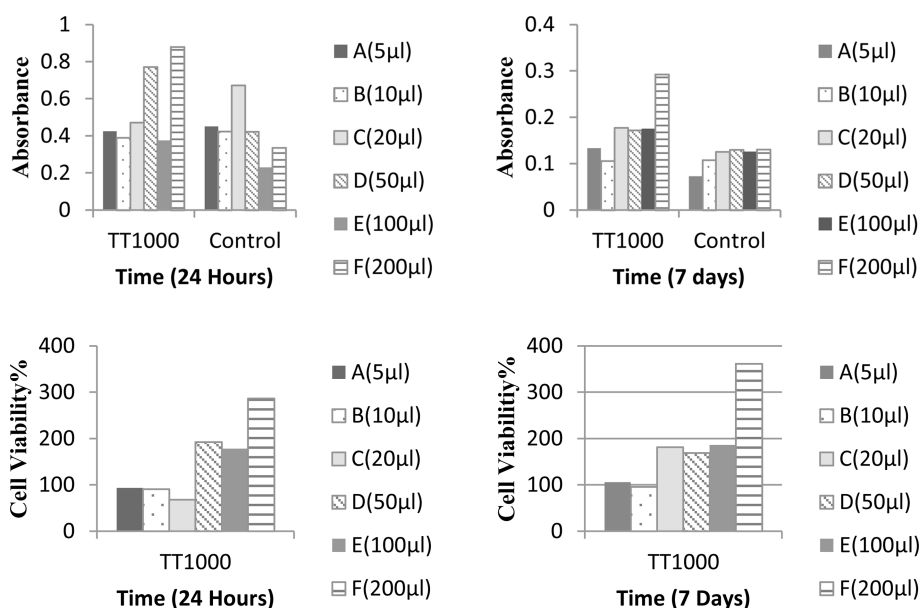


Fig. 13. Absorbance levels and cell viability of TT1000 in 24 hours and 7 days.

HCl. Therefore, it can react with calcium ions released from sample. This environment enables more dissolution to occur until it reaches to equilibrium stage comparing to deionized water. Due to the dissolution reactions in the Tris-buffer solution, H^+ and OH^- ions that released so pH of the solution changes. Fig. 12 indicates that pH of TT1000 increased excessively to 10.6. whereas, after 2 days pH remained almost the same. This can be attributed to fast dissolution of the material for the first two days.

Cell viability test

In-vitro cell viability test was conducted by seeding to SAOS-2 osteoblast-like cells at concentrations of 20 $\mu\text{g/ml}$, 50 $\mu\text{g/ml}$, 100 $\mu\text{g/ml}$ and 200 $\mu\text{g/ml}$ for 24 hours and 7 days. Fig. 13 indicates cell viability of the samples at different concentrations. ISO10993-5 standard represents that if the viability of treated human cell line culture is more than 70% means there is no toxic effect of the material [16]. According to ISO10993-5 standard, samples not only have non-toxic effect on the cells but also have the ability of cell adhesion, spreading, and results show increased viability over time. Highest cell viability was noted for the concentration of 200 μm .

Conclusions

β -TCP was produced from sea snail *Turritella terebra* via mechanochemical method. Bioactivity tests and SEM images indicate that the produced β -TCP was covered with HCA after immersing into SBF. Tris-buffer solution test results suggested that synthesized β -TCP is highly biodegradable.

Additionally, SBF studies showed a high bioactivity in the first week. MTT assay proposed non-toxic effect on SAOS-2 osteoblast-like cells. Along with their biological-natural origin, the costless *Turritella terebra* shells are attractive source for bioceramic production. On the other hand, the proposed mechanochemical conversion method is a simple and economic method in comparison to its analogues and guaranties nanoparticle

bioceramic production.

References

1. F. N. Oktar, H. Gokce, O. Gunduz, Y.M. Sahin, D. Agaogullari, I.G. Turner, L.S. Ozyegin, B. Ben-Nissan, Key Eng. Mater. 631 (2014) 137-142.
2. O. Gündüz, C. Gode, Z. Ahmad, H. Gökçe, M. Yetmez, C. Kalkandelen, F. N. Oktar, Journal Of The Mechanical Behavior Of Biomedical Materials 35 (2014) 70-76.
3. I. Karaca, O. Gunduz, L.S. Ozyegin, H. Gökçe, B. Ben-Nissan, S. Akyol, F. N. Oktar, Journal of the Australian Ceramic Society 54 (2017) 317-329.
4. Y. M. Şahin, O. Gunduz, B. Bulut, L.S. Ozyeğin, H. Gökçe, D. Alaogulları, F. N. Oktar, Acta Physica Polonica A. 127[4] (2015) 1055-1058.
5. J. H. G. Rocha, A.F.Lemos, S. Agathopoulos, P. Valério, S. Kannan, F.N. Oktar, J.M.F. Ferreira, Bone 37[6] (2005) 850-857.
6. K.-R. Kang, Z.-G. Piao, J.-S., In-A Cho, M.-J. Yim, B.-H. this chemical Kim, J.-S. Oh, J. S. Son, C. S. Kim, D. K. Kim, S.-Y. Lee, S.-G. Kim Implant Dent. 26[3] (2017) 378-387.
7. D. Kel, H. Gökçe, D. Bilgiç, D. Ađaođullary, I. Duman, M.L. Öveçođlu, E. S. Kayali, I. A. Kiyici, S. Agathopoulos, F.N. Oktar, Key Eng. Mater. 493-494 (2011) 287-292.
8. S. Agathopoulos, L.S. Ozyegin, Z. Ahmad, O. Gunduz, E.S. Kayali, O. Meydanoglu, F.N. Oktar, Key Eng. Mater. 493-494 (2011) 775-780.
9. O. Gunduz, Y. M. Sahin, S. Agathopoulos, B. Ben-Nissan, and F. N. Oktar, J. Nanomater. 2014 (2014) 1-6.
10. O. Gunduz, Y.M. Sahin, S. Agathopoulos, D. Ađaođullary, H. Gökçe, E.S. Kayali, C. Aktas, B. Ben-Nissan, F.N. Oktar, Key Eng. Mater. 587 (2013) 80-85.
11. T. Kokubo, H. Takadama, Biomaterials 27[15] (2006) 2907-2915.
12. B. Mehdikhani, G. Borhani, J. Ceram. Process. Res. 16[3] (2015) 308-312.
13. A. Sobczak-Kupiec, Z. Wzorek, R. Kijkowska, Z. Kowalski, Bull. Mater. Sci. 36[4] (2013) 755-764.
14. A. Ibrahim, W. Wei, D. Zhang, H. Wang, J. Li, Materials Letter 110(2013)195-197.
15. Bui, X. V., & Thang, T. D., ASEAN Journal on Science and Technology for Development. 33[2] (2016)38-68.
16. P. Sobierajska, A. Dorotkiewicz Jach, K. Zawisza, J. Okal, T. Olszak, Z. Drulis-Kawa, R. J. Wiglusz J. Alloys Compd. 748 (2018) 179-187.